

Seismic evidence for fluid migration accompanying subsidence of the Yellowstone caldera

Gregory P. Waite and Robert B. Smith

Department of Geology and Geophysics, University of Utah, Salt Lake City, Utah, USA

Received 24 April 2001; revised 20 November 2001; accepted 25 November 2001; published 10 September 2002.

[1] Seismicity of the Yellowstone volcanic field, northwest Wyoming, is characterized by swarms of earthquakes ($M_C < 3$) within the 0.64-Myr-old, 70 km by 40 km Yellowstone caldera and between the caldera and the eastern end of the 44-km-long rupture of the $M_S 7.5$ 1959 Hebgen Lake, Montana, earthquake. Over 3000 earthquakes with $M_C < 5$ were recorded during the largest historic swarm that spanned >3 months beginning in October 1985. The swarm had unusual characteristics indicative of interaction between seismicity and hydrothermal/magmatic activity: (1) the swarm followed the reversal of caldera-wide uplift of up to 1 m from 1923 to 1984 to subsidence; (2) swarm hypocenters occupied a nearly vertical northwest trending zone, and during the first month of activity, the pattern of epicenters migrated laterally away from the caldera at an average rate of 150 m/d; (3) the dominant focal mechanisms of the swarm were oblique-normal to strike-slip contrasting with the normal-faulting mechanisms typical of the region; and (4) the maximum principal stress axis averaged for the swarm events was rotated 90° from that of the normal background seismicity, from vertical to horizontal with a trend 30° from the strike of the plane defined by the swarm. We examined analytic models that best fit the focal mechanisms and the orientation of the plane defined by the swarm and found that the temporal shift of earthquake activity could be explained by the migration of hydrothermal fluids radially outward from the Yellowstone caldera following rupture of a sealed hydrothermal system within the caldera. *INDEX TERMS:* 7215 Seismology: Earthquake parameters; 7280 Seismology: Volcano seismology (8419); 8424 Volcanology: Hydrothermal systems (8135); 8434 Volcanology: Magma migration; *KEYWORDS:* volcano seismology, fluid migration, crustal stresses, seismicity and seismotectonics, hydrothermal systems

Citation: Waite, G. P., and R. B. Smith, Seismic evidence for fluid migration accompanying subsidence of the Yellowstone caldera, *J. Geophys. Res.*, 107(B9), 2177, doi:10.1029/2001JB000586, 2002.

1. Introduction

[2] The Yellowstone volcanic field is one of the largest and most active silicic volcanic systems in the world [Christiansen, 2001]. Yellowstone's youthful volcanic history is marked by three cataclysmic caldera-forming eruptions in the past 2 Myr. The youngest of these, at 0.64 Myr old, is called the Yellowstone caldera. Following the formation of the Yellowstone caldera, at least 30 rhyolite flows as young as 70,000 years old covered the Yellowstone area. This widespread volcanism is the main source of heat for the expansive hydrothermal system, which is manifest on the surface by geysers, hot springs, and fumaroles.

[3] The combined conductive and convective heat flux at Yellowstone is estimated to be an extraordinarily high 1800 mW/m^2 , which is 30 times the continental average [Fournier *et al.*, 1976]. The heat flow has been attributed in part to heat loss from crystallizing basaltic magma that feeds the

shallower rhyolitic magma systems and convection within Yellowstone's hydrothermal system [Fournier and Pitt, 1985].

[4] Yellowstone has experienced episodes of caldera-wide deformation including uplift of up to 1 m from 1923 to 1984 followed by a rapid change to subsidence that exceeded 25 cm to 1995 [Pelton and Smith, 1982; Holdahl and Dzurisin, 1991]. Following the deformation reversal, GPS measurements and interferometric synthetic aperture radar (InSAR) images revealed a partial return to uplift that continued to at least 2000, the time of last GPS observations [Wicks *et al.*, 1998; Meertens *et al.*, 2000]. Together, Yellowstone's widespread seismicity, high heat flow, and rapid changes in crustal deformation are the result of interaction between faults, hydrothermal and magmatic processes, and seismicity, the topic of this paper.

[5] The Yellowstone Plateau (Figure 1) is the most seismically active area of the 1300-km-long Intermountain Seismic Belt that extends from northern Montana to northern Arizona [Smith and Arabasz, 1991]. Further, it has experienced the largest historic earthquake in this region;

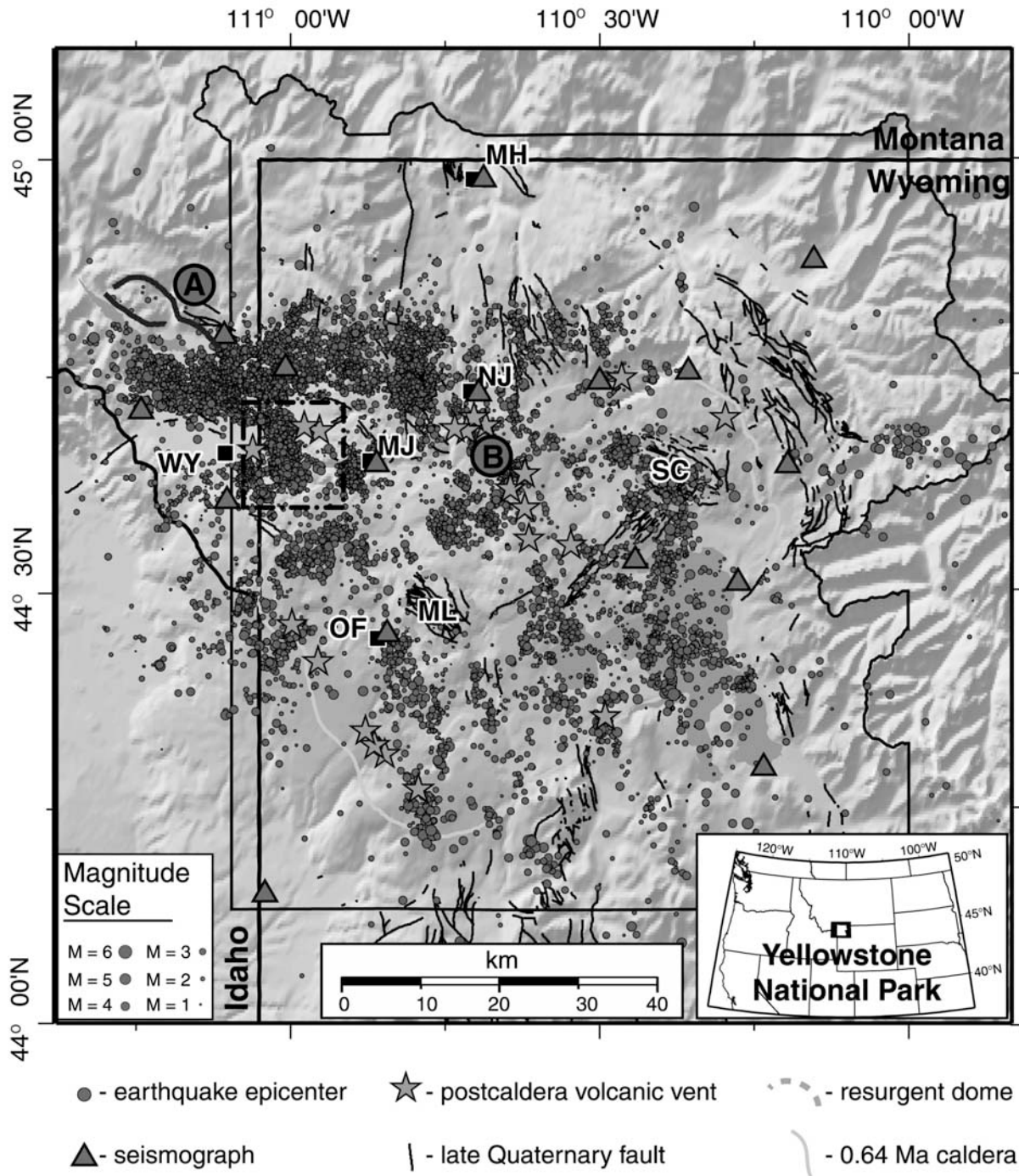


Figure 1. Yellowstone seismicity map: 1973–1997 (note that the network was not in operation from 1982 through late 1984). The Sour Creek (SC) and Mallard Lake (ML) resurgent domes are outlined with dashed blue lines. Place names are abbreviated MH, Mammoth Hotsprings; MJ, Madison Junction; NJ, Norris Junction; OF, Old Faithful; and WY, West Yellowstone. The rectangular region outlined with black is the region of the autumn 1985 swarm. Large circles mark the locations of the $M_S7.5$ 1959 Hebgen Lake (A) and $M_L6.1$ Norris Geyser basin (B) earthquakes. The surface rupture of the Hebgen Lake earthquake is shown as a maroon line. Figures 3 and 4 show the swarm sequence in more detail. See color version of this figure at back of this issue.

the August, $M_S7.5$ 1959 Hebgen Lake, Montana, earthquake, which had an epicenter ~25 km northwest of the Yellowstone caldera, developed an extensive aftershock zone east into and adjacent to the northwest side of the caldera. The fault scarp of this large earthquake extended to

within 20 km of the Yellowstone caldera and the 1985 earthquake swarm discussed here (Figure 1).

[6] Historical seismicity of Yellowstone, monitored since the installation of a permanent seismic network in 1973, is distinguished by spatial and temporal clusters of small,

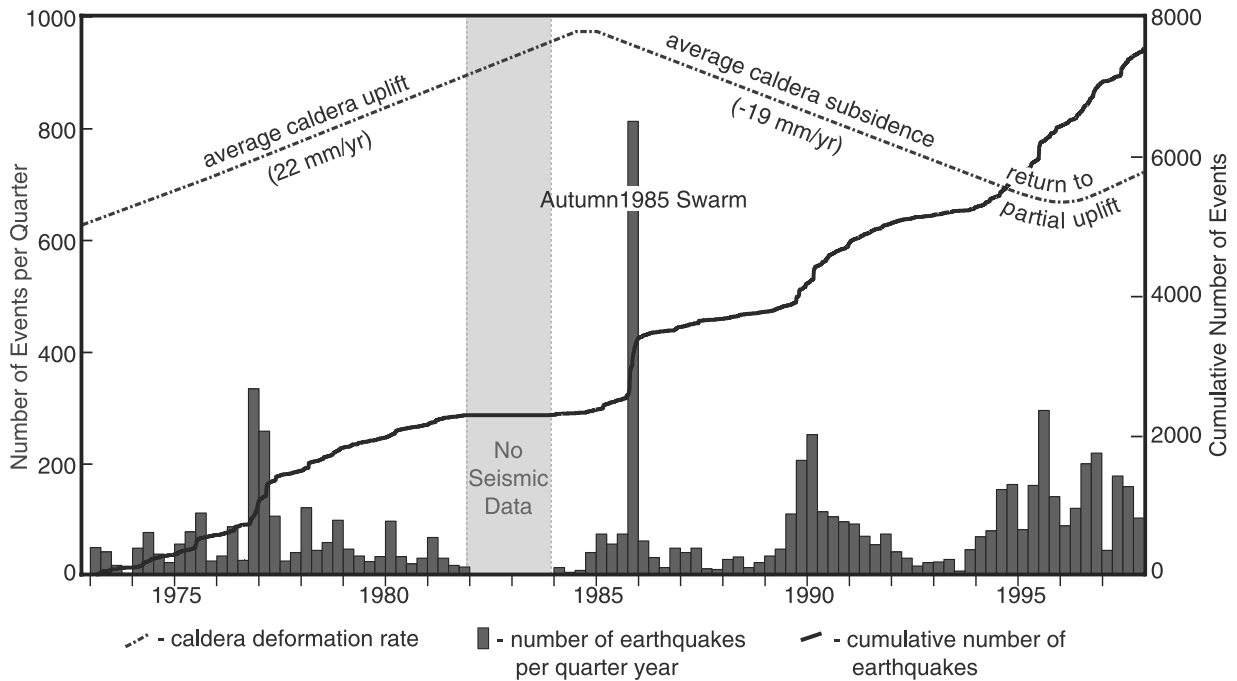


Figure 2. Time history of Yellowstone seismicity with a minimum magnitude cutoff of $M_C 1.5$. The average caldera deformation rates are from *Pelton and Smith [1982]* and *Dzurisin et al. [1994]*. The high seismicity in 1985 correlates with the reversal of crustal deformation from uplift to subsidence. The shaded area represents a period during which the seismic network in Yellowstone was not in operation.

shallow earthquakes, especially northwest of the caldera. A zone of densest seismicity extends from the Hebgen Lake area east to the northern caldera boundary near Norris Junction. Earthquake swarms in this area typically occur on east-west striking planes. The composite focal mechanisms from these sequences vary from normal faulting to strike-slip faulting with T axes generally perpendicular to the swarm planes. The epicenter of the $M_L 6.1$ 1975 normal-faulting earthquake near Norris Junction [*Pitt et al., 1979*], the largest historic intracaldera earthquake, was at the eastern end of this zone (Figure 1). It had a normal-faulting focal mechanism; however, the nodal planes had north-northwest strikes contrary to the east-west earthquake alignments in the rest of this zone [*Pitt et al., 1979; Bache et al., 1980*].

[7] Linear bands of seismicity within and adjacent to the caldera, some of which occurred as single swarms, are aligned north-northwest similar in orientation to the nodal planes of the 1975 Norris Junction earthquake. These lineations are parallel to alignments of postcaldera volcanic vents and regional faults. The orientations of these linear patterns are consistent with the Yellowstone Plateau's regional tectonic setting at the eastern edge of the extending Basin and Range tectonic province where the deformation measured by earthquake focal mechanisms, fault slip striations, and in situ measurements is generally east-west to northeast-southwest extension [*Zoback, 1992*]. Northwest trending volcanic rifts in the nearby Snake River Plain volcanic field are parallel to the alignments of volcanic vents in the Yellowstone caldera [*Smith et al., 1996*]. Similarly, GPS measurements show northeast-southwest extension across the Yellowstone caldera [*Meertens et al., 2000*].

[8] The temporal correlation between the largest historical earthquake swarm in Yellowstone and the unprecedented reversal in caldera deformation is the key observation (Figure 2) that motivated us in pursuing a study of the relation between seismicity and deformation. Our objective was to investigate the mechanism for the largest, most extensive, modern Yellowstone earthquake swarm and its relationship to hydrothermal and magmatic activity.

2. Volcanic History of Yellowstone

[9] The recent volcanic history of Yellowstone is defined by three cycles of silicic volcanic eruptions beginning 2.2 Myr ago, and we refer the reader to detailed record of the volcanic history recently published by *Christiansen [2001]*. Each of the three cycles began and ended with intermittent eruptions of rhyolite and climaxed with cataclysmic, caldera-forming, explosions. The caldera eruptions are estimated to have lasted only a few hours or days but expelled up to thousands of cubic kilometers of ash. These eruptions occurred at 2.0, 1.3, and 0.64 Myr ago.

[10] The most recent caldera eruption produced the Yellowstone caldera, a collapse basin 40 km by 70 km that was filled with postcaldera rhyolite flows and sediments. Two resurgent domes within the caldera, one in the southwest and one in the northeast, were elevated up to 500 m, indicating ongoing magma intrusion into the shallow crust (Figure 1). The youngest postcaldera flow occurred 70,000 years ago on the southern caldera rim [*Christiansen, 2001*]. Relatively minor eruptions of basalt occurred throughout the evolution of the first two eruption sequences, but basalts were generally erupted around the margins of the system. *Christiansen [2001]* suggests the denser basaltic magmas

were unable to reach the surface at the center of the system because of the less dense and nonrigid rhyolitic bodies in their path.

3. Geodetic Information on Caldera Deformation

[11] Precise, first-order leveling measurements of benchmarks on roadways revealed that the Yellowstone caldera began to subside between 1984 and 1985 after at least 61 years of net caldera-wide uplift of up to 1 m [Holdahl and Dzurisin, 1991]. The maximum uplift was measured near the center of the caldera ~ 30 km from the 1985 earthquake swarm discussed here. The first leveling survey was in 1923, but leveling was not repeated until 1975–1977. The significant uplift of up to 75 cm revealed by these repeat measurements [Pelton and Smith, 1982] prompted more frequent surveying within Yellowstone. Leveling surveys over a line that crosses the Sour Creek resurgent dome were repeated annually from 1983 to 1995, except 1994, and in 1998. These data show rapid uplift averaging 22 mm/yr during 1976–1984 followed by subsidence averaging -19 mm/yr beginning in 1985 [Dzurisin *et al.*, 1990]. This change from uplift to subsidence preceded the occurrence of the 1985 Yellowstone earthquake swarm by less than a year.

[12] Using GPS measurements, Meertens *et al.* [2000] noted a change in caldera deformation to local uplift in the vicinity of Norris Geyser basin between 1995 and 2000 after 10 years of subsidence within the caldera. We note that the second largest recorded swarm in Yellowstone occurred in this area in June 1995. In agreement with the GPS measurements, InSAR images by Wicks *et al.* [1998] show inflation in the area of Norris Geyser basin following the 1995 swarm. While this important coincidence is not discussed further in this paper, we present it as evidence for a possible relationship between well-sampled surface deformation observations and earthquake swarm activity.

[13] Unfortunately, there are no comparable geodetic data for the area of the 1985 Yellowstone swarm. Leveling lines were run along the road between West Yellowstone and Madison Junction that crossed the swarm area, but there are no surveys that bracket the swarm area closely in time and space [Holdahl and Dzurisin, 1991] (D. Dzurisin, personal communication, 2001). The 1984–1985 caldera-wide deformation reversal is well documented, but resolution of the geodetic data does not assist us in identifying a unique model for the autumn 1985 swarm.

4. Earthquake Data

[14] The seismic data used in this study are from the University of Utah, which has operated the Yellowstone Seismograph network since 1984. The U.S. Geological Survey operated the network between 1973 and 1981. During the autumn 1985 swarm, there were seven seismograph stations within 25 km of the swarm and 24 stations in the region including stations in the nearby Idaho National Engineering and Environmental Laboratory's network [Jackson *et al.*, 1993]. Hypocenters were located using the three-dimensional P wave velocity model of Miller and Smith [1999] derived by tomographic inversion of local earthquake and controlled sources. Average absolute hypocenter location errors for the 1985 swarm data are estimated

at ± 0.3 km in horizontal and ± 1.1 km in vertical at the 68% confidence interval. We caution the reader that because these error estimates are based on a linearized solution to a nonlinear problem, they may not represent the true errors in the solutions.

[15] For example, Lomax *et al.* [2000] tested earthquake location algorithms including a linear iterative method and an exhaustive nonlinear grid search technique on synthetic data to compare the locations and error estimates. They show that the linearized solutions' 68% confidence volumes may not agree with those of the grid search where the earthquakes lie outside the network or near strong velocity gradients. Further, when static noise was added to the travel time data to represent picking errors and/or near-station velocity model errors, these 68% confidence volumes did not contain the true solutions. While all of the earthquakes in the autumn 1985 swarm were within the network and had good azimuthal station coverage, we suggest the average confidence limits computed by location algorithm should be taken as a minimum.

5. Autumn 1985 Yellowstone Earthquake Swarm

[16] The largest historic earthquake swarm in Yellowstone occurred on the northwest rim of the Yellowstone caldera, 5–6 km east of the town of West Yellowstone, Montana (Figure 1). It began with a buildup of a few earthquakes per day on 4 October 1985 and continued with varying intensity over the next 3 months. More than 1800 events with $1.0 < M_C < 4.9$ and a total of 3156 events with $0.0 < M_C < 4.9$ were recorded and located by the University of Utah Seismograph Stations (M_C refers to coda magnitude used in routine earthquake reporting and is equivalent to M_L in this magnitude range). Undoubtedly there were many more small earthquakes that were not located. One hundred sixteen earthquakes were reportedly felt with Modified Mercalli Intensities (MMI) from II to V at locations within 5–10 km of the swarm in West Yellowstone and at Madison Junction (Figure 1) including three events on 9 November 1985 that shook West Yellowstone with MMI V [Hutchinson, 1986]. Many of the larger events were felt throughout Yellowstone Park, and the largest earthquake was felt as far away as Bozeman, Montana, more than 100 km to the north.

[17] By January 1986 most of the activity had subsided to a few events per day, but earthquakes continued to occur in the vicinity over the next several years. However, in the nearly 13 years of recorded seismicity prior to the swarm, there had been only ~ 100 located earthquakes in the area.

[18] The earthquake sequence was divided into three periods of activity based on the distribution of numbers of events per day (Figure 3): part I, 4 October through 8 November; part II, 9 November through 27 December; and part III, postswarm events from 28 December 1985 through 1986. A horizontal migration of hypocenters was observed during the first part of the swarm, followed by a possible gradual shift to deeper hypocenters over the course of the swarm and throughout the following year (Figures 3 and 4).

[19] During part I of the swarm, the number of earthquakes per day increased slowly to a peak of 197 events on 19 October and then gradually slowed to one earthquake on 7 November. The largest earthquakes were $M_C 3.5$ to $M_C 3.8$ and occurred during the middle of this period when the

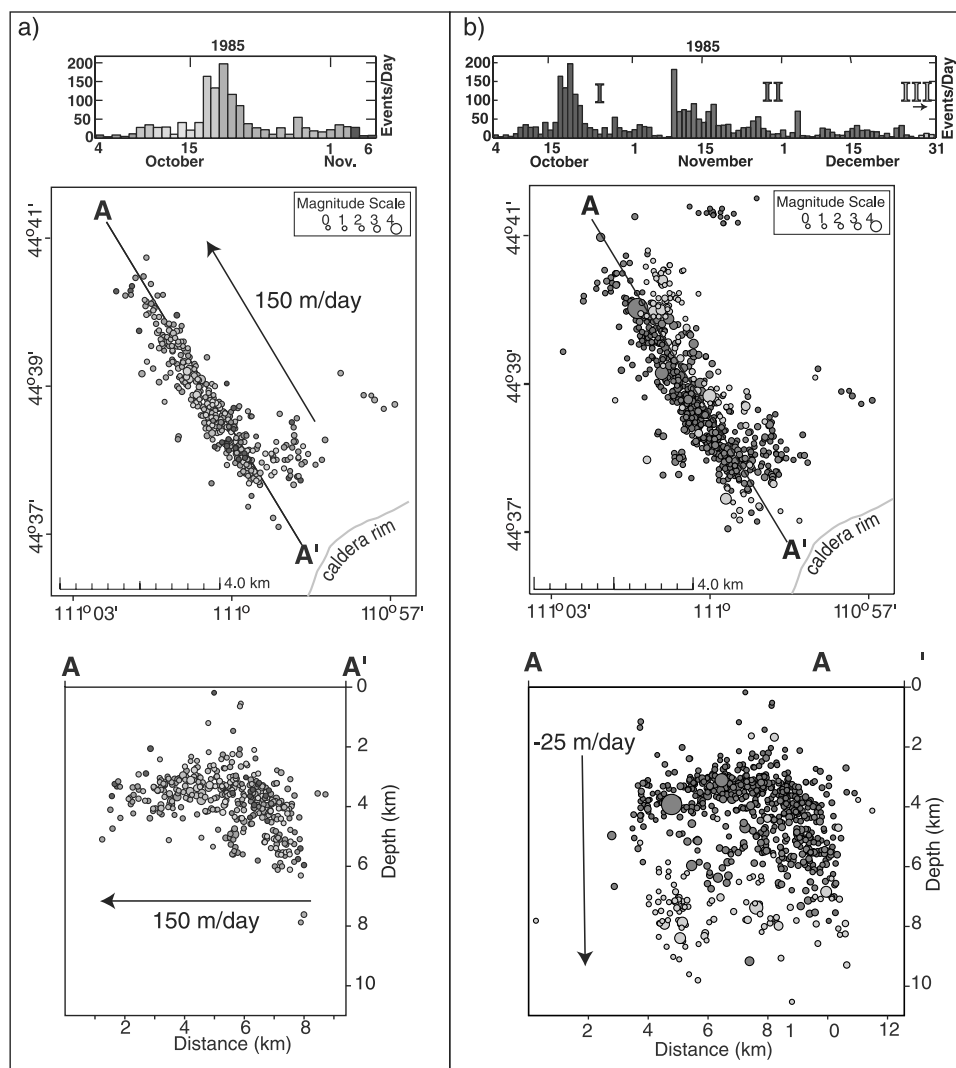


Figure 3. Earthquakes of the autumn 1985 Yellowstone swarm. Colors correspond to time periods shown in the bar graphs. (a) The initial month of the autumn 1985 earthquake swarm. Warm colors are earliest and cold colors are latest. Notice the general progression of the front of the swarm from southeast to northwest that is especially clear in the A-A' cross section with a 5-day flurry of activity beginning on 16 October. The rate of migration of activity is about 150 m/d. (b) All of the autumn 1985 swarm earthquakes. During the first month, shown in green, seismicity was relatively shallow. The red symbols correspond to the following month of activity during which events became systematically deeper. This second period began with two $M_C > 4$ events and decays similar to a main shock-aftershock sequence. The events shown in yellow continue on through 1986 in the same plane as the swarm and are the deepest. The downward migration occurred at a rate of about -25 m/d. See color version of this figure at back of this issue.

number of earthquakes per day was the greatest. The majority of the events were smaller than $M_C 2.5$, between ~ 2 and 5 km deep, and occurred in a 1-km-wide zone oriented N31°W. The size of the area defined by these events was ~ 20 km², which is approximately the rupture area of a $M_W 5.3$ earthquake [Wells and Coppersmith, 1994], whereas the maximum magnitude event during this period was $M_C 3.8$, which has a rupture area of < 1 km².

[20] The highest seismicity rates occurred over 4 days beginning on 16 October 1985 with 100–200 located earthquakes per day. There were also hundreds of smaller earthquakes each day that were not recorded at enough stations across the array for accurate locations. It was during

this period that most of the horizontal migration of epicenters took place. Earthquake activity migrated outward from a dense cluster at the edge of the caldera toward the northwest (Figures 3a and 4a). We measured the horizontal propagation rate by first computing the mean epicentral distance for a number of consecutive earthquakes to the nearest point on the caldera rim. A linear least squares fit to these mean values yielded the propagation rate. The rate of seismic activity propagation was ~ 150 m/d ($\sim 10^{-3}$ m/s) away from the caldera using bin sizes ranging from 25 to 100 earthquakes.

[21] Figure 4a shows the earthquake activity migration rate using bin sizes of 50 earthquakes. The bold solid circles

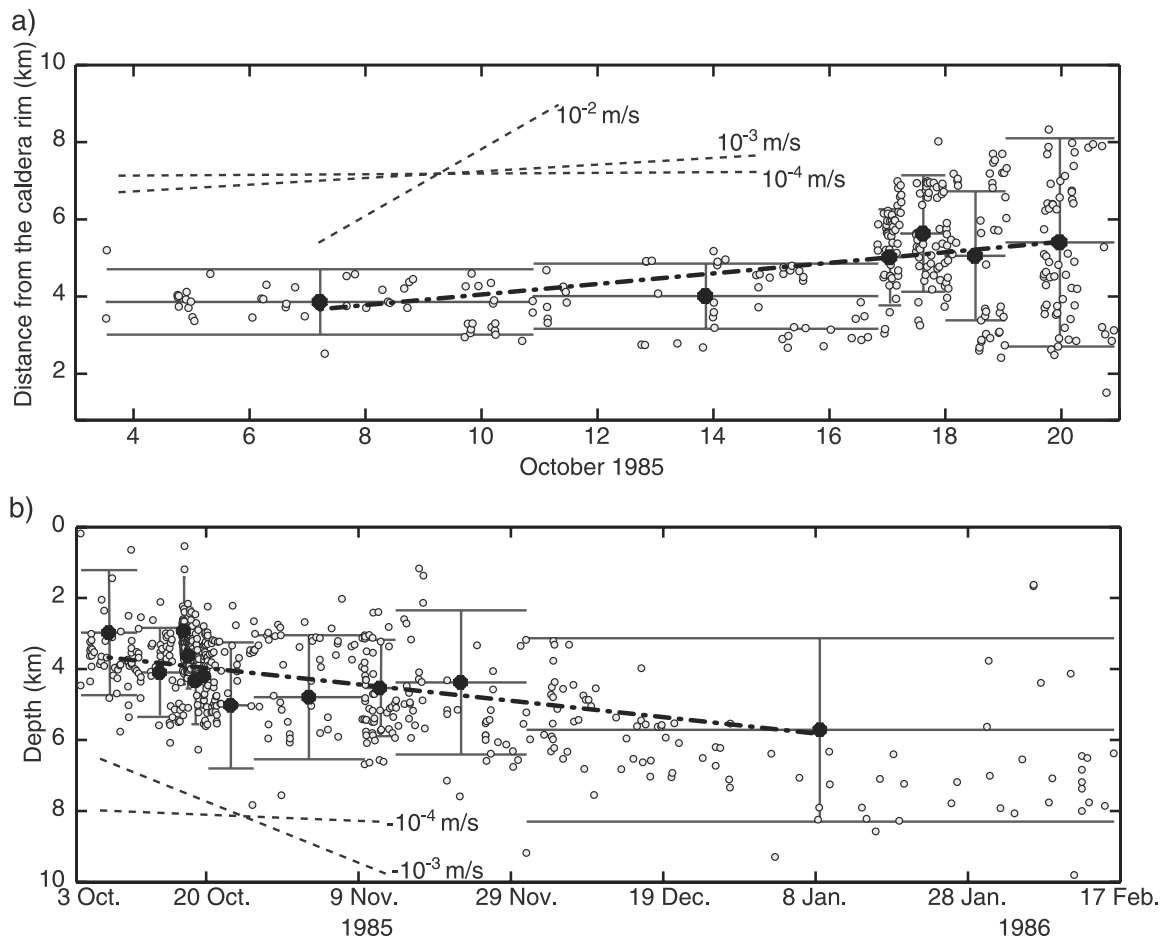


Figure 4. The 1985 Yellowstone swarm earthquakes (a) distance from the caldera and (b) depth as a function of time. The solid circles represent the mean distance/depth for groups of 50 earthquakes with $\pm 1\sigma$ shown with a thin solid line. The bold dash-dotted lines show the linear least squares fits to the means. Other rates are shown as dashed lines for reference.

represent the mean distance for each bin with corresponding standard deviation from that mean plotted as thin solid lines. Three rates are shown (thin dashed lines) for comparison with the best fit to the means.

[22] The Yellowstone swarm propagation rate is $\sim 1-2$ orders of magnitude lower than swarm propagation rates and dike intrusion rates observed in Hawaii and elsewhere. Reported rates vary over 3 orders of magnitude from >2 m/s for a vertical dike intrusion and eruption at Hekla volcano, Iceland [Linde *et al.*, 1993], to 10^{-2} m/s for a swarm on the Reykjanes Peninsula, Iceland [Klein *et al.*, 1977].

[23] Part II of the sequence began on 9 November with the largest earthquakes of the swarm: a $M_C 4.9$, $M_C 4.3$, and several $M_C > 3$ earthquakes occurred in addition to hundreds of smaller earthquakes. Many of these events were felt in nearby West Yellowstone, Montana. The zone of activity did not expand further horizontally during part II, but seismicity began to deepen as the rate of earthquake occurrence decreased (Figures 3b and 4b). Most of the seismicity was between 4 and 7 km deep. For the next several weeks the rate of earthquakes decayed similar to an aftershock sequence.

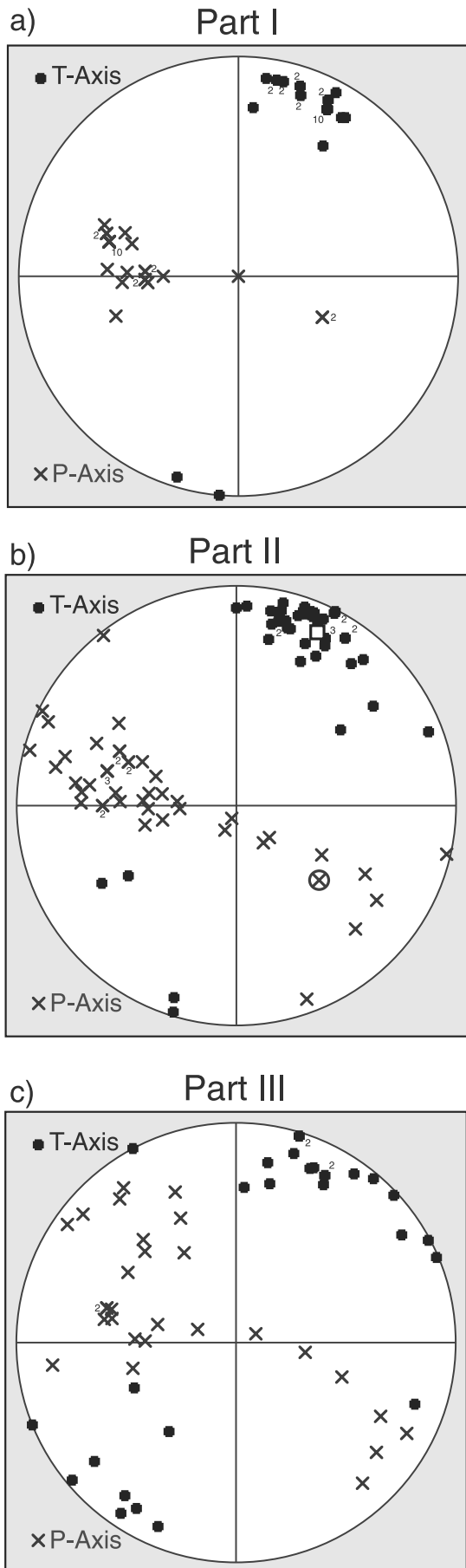
[24] Part III is defined by the earthquake activity that continued to occur at a lower rate throughout 1986 with

deeper foci in the same vertical zone. These small ($M_C < 3$) earthquakes generally occurred between 6 and 9 km deep.

[25] We used the technique described above for calculating the lateral migration rate during part I to calculate a vertical propagation rate over the duration of the swarm from 4 October 1985 through 17 February 1986. Using bin sizes ranging from 25 to 100 earthquakes, we found that swarm activity migrated at about -25 m/d. Given the vertical error in the hypocenter locations of at least ± 1.1 km this trend may not be significant; however, because vertical seismic activity migration has not been observed in other Yellowstone swarms, we felt it was important to investigate some possible causes for vertical swarm migration below.

5.1. Focal Mechanisms of Swarm Earthquakes

[26] Focal mechanisms of the 1985 swarm earthquakes were determined from P wave first motions using an automated algorithm [Reasenber and Oppenheimer, 1985]. Earthquakes from which focal mechanisms were computed were chosen according to the following criteria: An event must have at least eight clear, first-motion picks and the distance between the earthquake epicenter and the nearest station must be < 3 times the focal depth. Additional



constraints were used to eliminate poorly constrained mechanisms: solutions with a misfit >0.2 or an uncertainty in strike, dip, or rake $>30^\circ$ were removed. Focal mechanisms from 100 events made up the final set.

[27] The P and T axes for each focal mechanism are plotted in Figure 5. The data are separated based on the time periods described in section 4. The 28 focal mechanisms determined for part I of the swarm sequence were remarkably similar to one another. Seventy-five percent of the mechanisms were the same within the estimated errors in strike (7° error), dip (11° error), and rake (14° error). The dominant focal mechanisms were oblique-normal strike slip with the nodal planes striking $N75^\circ E$ and $N28^\circ W$ and dipping $50^\circ SE$ and $75^\circ NE$, respectively. The strike of this second steeply dipping nodal plane with left-lateral slip is parallel to the strike of the vertical plane containing the swarm earthquakes. The T axes are generally near horizontal, oriented north-northeast in each time period, but the P axes vary from shallow west-northwest plunge, through vertical to shallow southeast plunge after part I of the swarm. The 9 November $M_C 4.9$ event had an oblique-normal focal mechanism with nodal planes striking $N25^\circ W$ and $N87^\circ E$ and dipping $45^\circ SW$ and $69^\circ NW$, respectively. The P and T axes of this mechanism are highlighted in Figure 5b.

[28] All of the swarm earthquakes' first-motion focal mechanisms fit double-couple solutions, but there were almost twice as many compressional first arrivals as dilatational. This is suggestive of some mode I opening component in the earthquake source mechanisms but may simply be the result of the geometry of the stations with respect to the swarm. This study used only P wave first-motion focal mechanisms, so we have no information about nondouble-couple components of the seismic sources, such as net volume changes. We also point out that long-period earthquakes, common in many other volcanically active regions, were not identified in this swarm and, in fact, have not been reliably observed at Yellowstone.

5.2. Swarm Stress Inversion

[29] *Gephart and Forsyth's* [1984] focal mechanism stress inversion program was used to determine the direction of the principal stress axes from the focal mechanisms of the swarm earthquakes. The assumptions used in this method are that the stress is homogeneous in the region of study and that earthquakes do not alter the stress field. It also assumes that slip occurs in the direction of maximum resolved shear stress. The algorithm uses a grid search over possible orientations of the principal stresses and ratio of stress magnitudes ($R = (\sigma_2 - \sigma_1)/(\sigma_3 - \sigma_1)$) and determines the maximum resolved shear stress for each orientation. Each focal mechanism is compared to the predicted model at each grid point and the minimum rotation angle, or misfit,

Figure 5. (opposite) P and T axes from earthquake mechanisms for each of the three parts of the 1985 Yellowstone swarm (see text). The P and T axes of the 9 November 1985 $M_C 4.9$ earthquake are shown as a circled cross and open square, respectively. Numbers next to some symbols indicate the number of P or T axes with the same orientation.

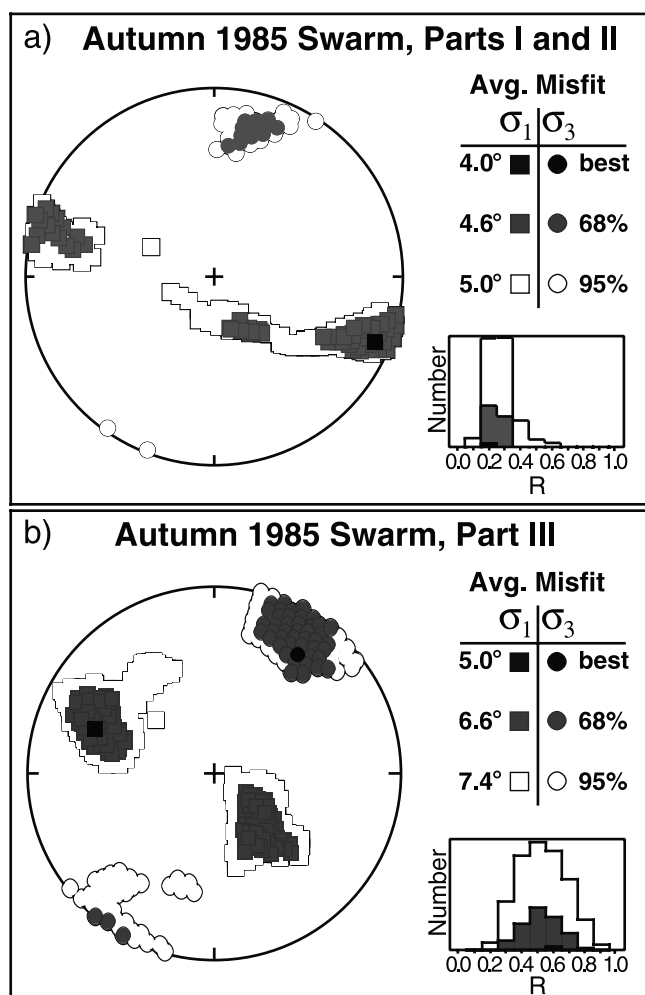


Figure 6. Maximum and minimum principal stress axis directions from stress inversion of focal mechanisms of the autumn 1985 Yellowstone swarm. (a) The inversion of 72 swarm earthquake focal mechanisms (parts I and II). (b) The inversion of 28 postswarm earthquake focal mechanisms (part III). Table 1 lists the best fit orientations for the three principal stresses.

between the predicted and observed slip direction is calculated. The configuration of stress directions with the smallest average misfit for the entire data set is determined to be the best fit solution. The inversion results for the 1985 Yellowstone swarm earthquakes and postswarm earthquakes are shown in Figure 6 and summarized in Table 1. Figure 6 shows the best fit solution for σ_1 and σ_3 along with the range of solutions within the 68% and 95% confidence ranges.

[30] The stress inversion for the 72 events that occurred during the swarm (parts I and II) have a best fit solution with σ_1 plunging 9° , S68°E, 30° from the trend of the swarm, and σ_3 plunging 17° , N19°E (Figure 6a). This best model had a low misfit of 4.0° , but there is considerable scatter in the range of acceptable solutions for σ_1 at the 95% confidence level. This may be explained by the low values found for the ratio R . For a normal faulting stress regime, $R = 0$ implies $\sigma_1 = \sigma_2$, and the predicted deformation is oblique normal to pure strike slip [Zoback, 1989]. The low

values for R in the 68% confidence range of 0.2 and 0.3 indicate σ_1 and σ_2 are close in magnitude and agree with the observed predominance of oblique strike-slip focal mechanisms. The maximum principal stress orientation is consistently vertical elsewhere in the extensional Yellowstone region, but it was rotated to horizontal during the 1985 swarm.

[31] The best fitting stress model of the postswarm focal mechanism data (part III) has σ_1 plunging 33° , N70°W, while σ_3 remained in roughly the same orientation as it was during the swarm plunging 23° , N36°E (Figure 6b). In this case, there are two distinct regions of σ_1 orientations at the 95% confidence level, which may reflect heterogeneity in the area. Some of these deeper postswarm earthquakes seem to have responded to the same stresses as those that caused the swarm events, but the steeper plunging solutions for σ_1 indicate a return to normal faulting. The higher misfit of 5.0° is due to the wider variation in postswarm mechanism types. There is a wide range of values for R in part III, from 0.2 through 0.9 at the 95% confidence level but a peak near 0.5 and a best fit value of 0.6. The higher R values support the interpretation of a transition back to normal faulting.

6. The 1985 Earthquake Swarm Mechanics

[32] The earthquakes that occurred during the first part of the autumn 1985 swarm had characteristics that are unique among earthquake swarms at Yellowstone. The first is the migration of earthquake activity from the caldera rim outward to the north-northwest that occurred at a rate of ~ 150 m/d (Figure 4a). No other Yellowstone swarms have revealed this type of migration behavior, radially away from the caldera.

[33] The second unique feature is the concomitant change in caldera deformation from decades of uplift to subsidence. The third characteristic is the departure from normal-faulting earthquakes to swarm earthquake mechanisms, which were oblique normal and the corresponding change in the orientation of the maximum principal stress axis. The composite focal mechanisms of most Yellowstone swarms have a near-vertical P axes. However, the maximum principal stress axis of the first part of the autumn 1985 swarm was rotated from its typical vertical direction to nearly horizontal and 30° from the direction of swarm elongation. The minimum principal stress direction was horizontal and 60° from the strike of the swarm plane, similar to other Yellowstone swarms where the orientation of the T axes were at high angles to the swarm planes.

[34] Before discussing specific models for the autumn 1985 Yellowstone swarm, we note the influence the largest historic earthquake in the Rocky Mountains had on the state of stress in the vicinity of the swarm. The T axes from the dominant swarm events' focal mechanisms are similar in

Table 1. The 1985 Yellowstone Swarm Principal Stresses^a

Time Period	N	σ_1		σ_2		σ_3		R	ϵ
		Pl	Tr	Pl	Tr	Pl	Tr		
Parts I and II	72	9°	S68°E	70°	S49°W	17°	N19°E	0.2	4.0
Part III	28	33°	N70°W	48°	S26°E	23°	N36°E	0.6	5.0

^aN, number of earthquakes; Pl, plunge; Tr, trend; R, ratio of stress magnitudes (see text); ϵ , average misfit.

orientation to the T axis computed from the normal-faulting Hebgen Lake earthquake by *Doser* [1985], and although 26 years separate the 1959 $M_S7.5$ Hebgen Lake earthquake and the 1985 swarm, geodetic measurements [*Meertens et al.*, 2000] across the fault reveal that north-northeast extension perpendicular to the fault continued through 2000.

[35] In addition, the location and orientation of the plane of swarm events are roughly aligned with the southeastern end of the Hebgen Lake earthquake surface rupture (Figure 1). *Chang and Smith* [2002] modeled the Coulomb stress changes induced by the Hebgen Lake earthquake and found a lobe of increased failure stress for planes oriented subparallel to the plane defined by the autumn 1985 Yellowstone swarm. While the focal mechanism for the Hebgen Lake earthquake has a vertical P axis and stress inversion solutions computed from the swarm earthquake focal mechanisms have a near horizontal σ_1 , the coseismic and post-seismic extension of the Hebgen Lake fault zone is subparallel to the direction of extension inferred from the 1985 swarm events. This extension may have controlled the orientation of the 1985 swarm.

6.1. Lateral Swarm Migration

[36] Horizontal spatial-temporal shifts in seismicity have been observed in volcanic areas and occasionally in non-volcanic regimes worldwide on similar timescales and spatial scales as reported here [e.g., *Hill*, 1977; *Rubin et al.*, 1998]. The horizontal migration of earthquake activity during the autumn 1985 swarm is consistent with earthquake triggering by propagation of a hydrothermal or magmatic fluid. The initial ~ 150 m/d horizontal migration and perhaps the longer-term deepening of earthquake activity are likely to be related to fluid movements. We investigated three models that involve the migration of hydrothermal or magmatic fluids to induce earthquakes.

[37] Although there have been no eruptions of lava at Yellowstone in the past 70,000 years [*Christiansen*, 2001], this does not preclude the possibility that magma may flow in dikes not yet erupt. In fact, most episodes of unrest at large calderas do not lead to eruptions [*Newhall and Dzurisin*, 1988], and the probability of a dike reaching the surface is only a small fraction of the probability of dike injection from the source magma chamber [*Gudmundsson et al.*, 1999].

[38] A few examples of possible dike intrusions that did not lead to surface eruptions include the 1980 earthquakes [*Julian and Cockerham*, 1982] and the 1989 swarm at Long Valley caldera, California [*Hill et al.*, 1990], the 1997 swarm off the Izu Peninsula, Japan [*Yosuke et al.*, 1999], and numerous events at Kilauea caldera, Hawaii, and Krafla Volcano, Iceland [e.g., *Rubin and Pollard*, 1987].

[39] In addition, *Kumagai et al.* [2001] report that the gradual deflation of the caldera on Miyake Island, Japan, coincided with an elongated earthquake swarm northwest of the volcano. They modeled the caldera collapse as a descending vertical piston of solid materials in the conduit and magma chamber of the volcano accommodated by magma flowing from the magma chamber. *Kumagai et al.* [2001] suggest that the magma outflow may have caused the earthquake swarm and note that no eruptions of large amounts of magma were associated with the caldera formation

[40] Several lines of evidence including a large negative gravity anomaly, the extraordinarily high heat flow and

seismic tomographic imaging, suggest there is magma at midcrustal depths beneath Yellowstone [e.g., *Smith et al.*, 1974; *Eaton et al.*, 1975; *Fournier and Pitt*, 1985; *Savage et al.*, 1993; *Dzurisin et al.*, 1994]. *Miller and Smith* [1999], using local earthquake tomography, give the best direct evidence. They interpret a crustal volume in the southwestern part of the caldera that has low P and S wave velocities, compared to surrounding areas, coupled with relatively high ratios of P to S velocities as a zone of 10–30% partial melt. The top of this zone is 6–8 km beneath the caldera, and it extends to depths of at least 16 km. The location of this active magma system is 15 km southeast of the 1985 earthquake swarm. Further, a second low-velocity volume may represent a zone of partial melt beneath the northeast part of the caldera near the Sour Creek resurgent dome [*Miller and Smith*, 1999]. The locations of these low-velocity volumes are coincident with the sources of caldera deformation modeled from geodetic data [*Vasco et al.*, 1990].

[41] We note that *Savage et al.* [1993] proposed a model for crustal deformation in which an expanding vertical dike extending from the Sour Creek resurgent dome to the Hebgen Lake region was responsible for the observed northeast crustal extension in that region. Similarly, we acknowledge that shallow, propagating magma could have been responsible for triggering the autumn 1985 swarm.

[42] The range and magnitude of the hydrothermal fluid system in Yellowstone are unique among active silicic volcanic complexes. The extensive geysers and hot springs of Yellowstone provide ample evidence of high-temperature water circulation through the upper crust so the influence of hydrothermal fluid migration on earthquake occurrence must be examined as well.

[43] Examples of documented changes in the hydrothermal systems in Yellowstone that were correlated with other earthquake swarms include (1) increased geyser activity, (2) changes in the clarity and temperature of water in hot springs, and (3) formation of new fumaroles and mud caldrons [e.g., *Pitt and Hutchinson*, 1982]. In addition, a steam explosion produced a large crater on the east side of the caldera several months prior to the 1985 Yellowstone swarm and a 150 m² crater formed from an explosion 15 km northeast of the swarm in January 1986 [*Dzurisin et al.*, 1994]. Similar postglacial hydrothermal explosion craters ranging in diameter from 10 to 1500 m have been found throughout the Yellowstone caldera [*Muffler et al.*, 1971].

[44] The migration of seismic activity observed during the first few weeks of the autumn 1985 swarm, is not considered unusual for swarms in other volcanic areas. *Hill* [1977] proposed an explanation for swarm migration based on a model of a cluster of dikes oriented with their long dimensions parallel to the regional maximum principal stress, σ_1 . Shear failure occurs along oblique fault planes connecting adjacent tips of en echelon or parallel dikes when a critical combination of fluid pressure ($P > \sigma_3$) in the dikes and difference between σ_1 and σ_3 is reached. Slip on a particular fault will result in an incremental volume increase in the immediate vicinity and subsequent fluid pressure drop in adjacent dikes. This will stabilize the immediate system of dikes and fractures but will perturb the stress field in neighboring dikes triggering earthquakes in those systems. The stress perturbation in the adjacent dikes could induce

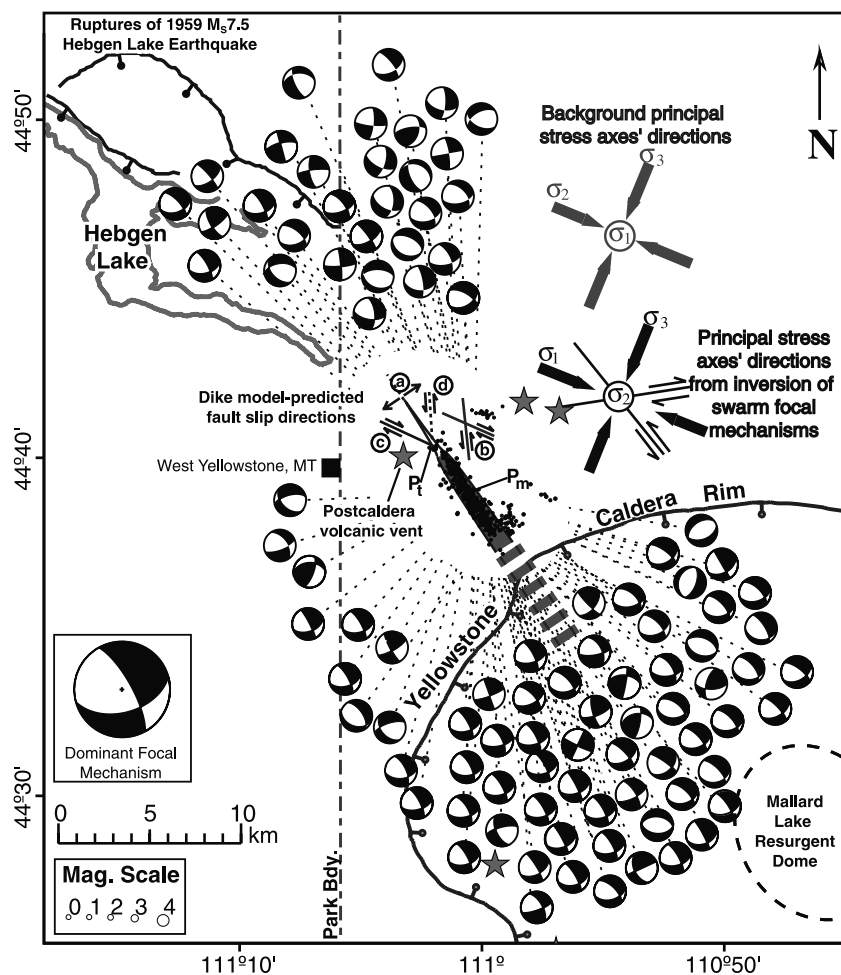


Figure 7. Focal mechanisms determined for the autumn 1985 Yellowstone swarm with hypothetical dike originating within the caldera. The width of the dike is greatly exaggerated. P_m is the magma pressure and P_t is the fluid pressure in the cavity at the tip of the dike. Four types of deformation predicted by *Rubin's* [1995b] and *Rubin and Gillard's* [1998] dike intrusion models are possible: type a, Mode I crack opening; type b, slip on existing faults away from the tip cavity; type c, slip on existing faults adjacent to the tip cavity; and type d, shear failure of intact rock adjacent to the tip cavity. The background principal stress axes' directions are from an inversion of focal mechanisms in the area surrounding the 1985 swarm that did not include the swarm earthquakes. Note the 90° rotation of σ_1 and σ_2 from the background state of stress to the swarm stress field. Stars indicate the locations of postcaldera volcanic vents.

the same type of earthquakes and the stress field perturbation would propagate away from the initial site of activity. In this model, earthquake activity migrates as a result of the stress perturbation and does not require transfer of fluids. However, the fluid pressure must overcome the least compressive stress so that the dike can dilate.

[45] In the case of the 1985 Yellowstone swarm, *Hill's* [1977] model predicts a system of en echelon dikes with their long dimensions oriented west-northwest, parallel to the direction of σ_1 revealed by the stress inversion. In order to match the locations of the earthquake epicenters a system of dikes requires a geometry similar to the systems of eruptive fissures at Kilauea, Hawaii, and dikes inferred from an earthquake swarm on the Reykjanes Peninsula, Iceland, described by *Hill* [1977]. The conjugate faults could be a series of oblique strike-slip faults striking approximately $N30^\circ W$ and $N75^\circ E$ to match the strikes of

the dominant focal mechanisms. Increased fluid pressure from within the caldera could initiate the swarm by encouraging slip on adjacent faults which would propagate the perturbation away from the caldera. The fluid that fills the cracks in this model could be either magma or water.

[46] Models by *Rubin* [1995b] and *Rubin and Gillard* [1998] for dike swarms in Hawaii and Iceland were also examined as possible models for the 1985 Yellowstone swarm. Figure 7 shows a schematic diagram for four types of deformation induced by dike propagation due to excess source pressure adapted from *Rubin* [1995b]: Mode I crack opening induced by the excess magma pressure (Figure 7, type a); slip on suitably oriented existing faults away from the tip cavity and adjacent to the tip cavity (Figure 7, types b and c); and shear failure of intact rock adjacent to the tip cavity (Figure 7, type d). The dike is under uniform horizontal normal stress, σ_3 and source magma pressure,

P. Fluid pressure in excess of the normal stress ($P > \sigma_3$) induces crack opening. The cavity at the tip of the dike has no magma in it and has a fluid pressure $P_t < \sigma_3$. This constraint ensures that the tip cavity will have a suction effect on the crack and will prevent the crack from propagating at elastic wave speeds [Rubin, 1995b].

[47] In general, shear slip occurs on optimally oriented faults ($\sim 30^\circ$ from σ_1 for a coefficient of friction of 0.6) when the ratio between the greatest compressive stress and the least compressive stress exceeds a value determined by the coefficient of friction on the fault surface. In order to produce fractures of intact rock the compressive strength of the rock must also be overcome. This requires a greater perturbation of the ambient stress field than does shear sliding on favorably oriented faults. The stress changes induced by a propagating dike are small enough that the production of earthquakes larger than magnitude 1 or 2 requires a large enough ambient differential stress that the earthquake focal mechanisms should be consistent with the background stress field [Rubin, 1995b].

[48] If we accept this model for the autumn 1985 Yellowstone swarm, we see that the ambient stress field must have had a significant effect on the swarm. For example, the direction of the minimum principal stress, σ_3 during the swarm remained consistently north-northeast in the same orientation as the regional σ_3 direction and 60° from the orientation of the swarm instead of perpendicular to the swarm as predicted by the model. The rotation of σ_1 may have occurred in response to increased horizontal pressure from a magma source presumably within the caldera. As indicated by the low stress magnitude ratio, *R*, the magnitudes of σ_1 and σ_2 are about equal so a small increase in the horizontal pressure may have been enough to cause the rotation of σ_1 and σ_2 .

[49] The dominant mechanisms during the swarm were oblique-normal strike-slip events with one steeply dipping nodal plane striking N28°W parallel to the direction of swarm elongation. This is about 30° from the σ_1 direction. Figure 7 shows the focal mechanisms together with the orientation of a hypothesized dike. The position of the dike is based only on the earthquake locations since there are no other data to constrain it. The principal stress directions are 35° to 40° from those predicted by Rubin's [1995b] model for a dike of this orientation. These are considerable deviations from the theoretical model, but the ambient stress field and/or the preexistence of a fault zone could favor faulting in that direction over orientations closer to the predictions as noted by Rubin [1995b].

[50] We estimate the type of fluid that could be found in such a dike based on the range of plausible viscosities as determined by the propagation rate and dimensions of the swarm plane. The uncertainties in the temperature of the host rock, host rock composition, source pressure, and dike-fluid temperature suggest viscosity estimates that range over two orders of magnitude, but fluid viscosity variations are much greater: rhyolite melt viscosity varies from 10^4 to 10^8 Pa s, the viscosity of basaltic melt varies from 10 to 10^2 Pa s [Rubin, 1995a] and the viscosity of water is on the order of 10^{-3} Pa s.

[51] If we assume the fluid is magma, we can estimate the viscosity based on the length of time it took for the dike to propagate. A magmatic dike with a melt temperature of

1300°C intruded into a host rock with a temperature of 200°C would have to be at least 3 m thick to avoid freezing completely in the 17 days during which the migration of swarm activity occurred based on Rubin's [1995b] equation (14):

$$w = 2\lambda\sqrt{\kappa t}, \quad (1)$$

where w is the width of the frozen margin between the host rock and the magma, κ is the thermal diffusivity of the host rock (1.5×10^{-6} m²/s), and t is time (17 days). We equate the frozen margin thickness to the half width of a solidified dike. The dimensionless parameter λ depends on the magma and host rock temperatures, the latent heat of crystallization, and the heat capacity [see Carslaw and Jaeger, 1959]. For a basaltic dike intruded into a granitic host rock, $\lambda \approx 0.5$. A lower-temperature rhyolite dike would have to be at least 5 m wide to avoid freezing in 17 days and would have $\lambda \approx 0.9$.

[52] We estimate the fluid pressure necessary to produce a 3-m-wide opening over half the length of the dike (2 km) is on the order of 10 MPa by rearranging Rubin's [1995b] equation (1):

$$\Delta P = \frac{w\mu}{\lambda(1-\nu)}, \quad (2)$$

with ΔP equal to the magma pressure minus the compressive stress, μ is the elastic shear modulus of the host rock (2.5×10^{10} Pa), and ν is Poisson's ratio of the host rock (0.18). The pressure gradient is estimated from the excess pressure divided by the half length of the dike and is used to estimate the viscosity of the fluid, η , by combining Rubin's [1995b] equations (3) and (6):

$$\eta = \frac{\omega^2}{3\dot{u}_x} \frac{d\Delta P}{dx}, \quad (3)$$

where \dot{u}_x is the horizontal velocity (150 m/d) and we have neglected horizontal gradients in vertical and tectonic stresses. A 3-m-wide dike of basaltic melt requires a viscosity on the order of 10^6 Pa s, which is 4 orders of magnitude too high for a basalt. A wider rhyolitic dike, however, requires a viscosity on the order of 10^7 Pa s, which agrees with published values for rhyolite viscosity.

[53] If the Yellowstone swarm was caused by propagation of a magma-filled crack, the composition of the magma was most likely rhyolite. However, in an analysis of the propagation of rhyolite dikes, Rubin [1995a] suggests that it is much more difficult for rhyolite dikes to propagate versus basaltic dikes because of the higher viscosity. Rhyolite dikes with shallow sources are impeded by the large temperature contrast between the dike and the host rock as well.

[54] The thermal-physical properties of water are much different from magmas, so this analysis does not apply in the same way, but we suggest that a water-filled dike would not fit the observations. From equation (3) we can see that the width at the center of a water-filled dike must be on the order of 1 mm or less and thus the excess fluid pressure on the order of a kilopascal to match the observed propagation velocity of the seismic activity. In this case we can not ignore horizontal stress gradients due to vertical and tectonic stresses as they may be larger than the driving pressure

gradient which is only on the order of a pascal. *Rubin's* [1995b] dike model would probably not apply since the main source of any stress change would be poroelastic rather than the direct stress perturbation due to the crack. A more likely mechanism for induced seismicity due to the migration of hydrothermal fluids is given below.

[55] *Fournier* [1999] suggests a model for the possible relationship between the changes in the hydrothermal systems and earthquake swarms which does not require fluid pressure greater than the least compressive stress. The migration of hydrothermal fluids, possibly due to pressure and temperature changes in the magma chamber or below a hypothesized self-sealed hydrothermal layer, may induce earthquakes on favorably oriented fractures by increasing the pore fluid pressure. A slight increase in pore pressure could reduce the effective normal stress on the fracture planes enough to allow a fault to slip. In addition, an increase in seismicity could expand the plumbing system of a particular hydrothermal area, permitting convective fluid flow in a larger area [Pitt and Hutchinson, 1982].

[56] In the case of the 1985 swarm a hypothesized self-sealed layer may have ruptured to release hydrothermal fluids and induce earthquakes on favorably oriented fractures. *Dzurisin et al.* [1994] propose that the caldera's subsidence is attributed to depressurization and fluid loss from the deep hydrothermal system and sagging of the caldera floor in response to regional crustal extension. They suggest that earthquakes may trigger such a depressurization by rupturing a layer that normally seals in the fluids derived from magma degassing. Another process that may rupture a self-sealed layer is accumulation of these magma-derived fluids until a self-sealed layer is sufficiently stretched to rupture by tensile failure [Fournier, 1999]. A similar mechanism involves increased pressure associated with an episodic pulse of magma from below and subsequent tensile failure of the layer [Fournier, 1999].

[57] After breaching a self-sealed layer the fluids may have migrated outward to the northwest and caused the 1985 swarm earthquakes. This fluid migration would have most likely occurred as pulse of increased pore fluid pressure along preexisting cracks. The similarity of the orientations of the steeply dipping nodal plane of the dominant focal mechanisms and the plane containing the swarm earthquakes suggests the swarm could have occurred as a repeated propagating fracture along a single plane or closely spaced parallel planes.

[58] In order to determine whether the rate of migration of the seismic front is reasonable for hydrothermal fluids, we estimate the hydraulic diffusivity using a method from *Talwani and Acree* [1985], who investigated earthquakes associated with reservoir filling. They find the hydraulic diffusivity from the "seismic diffusivity" given by the distance the seismic front traveled, L , and time, t , as $D_S = L^2/t$. *Talwani and Acree* [1985] argue that this estimate should be within an order of magnitude of the hydraulic diffusivity. The migration of earthquake activity during the first part of the autumn 1985 swarm covered a distance of 4 km over a period of 17 days giving $D_S \approx 10 \text{ m}^2/\text{s}$. On the basis of seismicity induced by reservoir impoundment, *Talwani and Acree* [1985] calculated diffusivity estimates ranging from 0.5 to 50 m^2/s and *Simpson et al.* [1988] calculated estimates of 1–10 m^2/s .

[59] The agreement with these published estimates indicates that the propagation of hydrothermal fluids from the caldera is a reasonable explanation for the migration of the 1985 Yellowstone swarm activity. These rates are orders of magnitude higher than expected for bulk rock based on laboratory measurements, so the diffusivity must be controlled by large-scale preexisting fractures [Simpson et al., 1988]. The existence of preexisting fractures may be especially important in the case of the Yellowstone swarm as the diffusion estimate was at the high end of the range given by *Simpson et al.* [1988].

[60] While the estimate of the diffusivity for the Yellowstone swarm is in agreement with these published values, we caution that it may not be analogous to reservoir-induced seismicity due to the different mechanisms by which the pore pressure is increased. For example, *Sasaki* [1998] showed that induced seismicity depends strongly on the injection flow rate and wellhead pressure in a study of hydraulic fracturing-induced seismicity at Hijiori geothermal site, Japan.

[61] We summarize the plausible models for such a fluid induced swarm in Figure 8. If magmatic, the fluid may have originated at the inferred magma chamber that lies beneath the caldera at a depth of ~ 8 and 15 km to the southeast of the swarm. A brine may have originated within a shallower self-sealed layer. Fluid moved upward and outward to the northwest through hot crustal material producing no measurable earthquakes. Measurable earthquakes began to occur as the fluid traveled into the shallow brittle crust outside the caldera. Earthquakes that occurred before the swarm (1973 to September 1985) are plotted in light shaded and those that occurred during the first month (part I in Figure 3) of the swarm are plotted as solid dots. The brittle-ductile transition was estimated from the maximum depth of earthquakes [Smith et al., 1998].

6.2. Vertical Swarm Migration

[62] The shift to greater hypocentral depths with time during the autumn 1985 swarm is difficult to understand, as one would expect upward migration of fluids due to buoyancy. Typically, dikes propagate to shallower depths and induced seismicity shallows with time. We note, however, that *Rubin et al.* [1998] observed deepening of activity with time during a January 1983 dike intrusion at Kilauea Volcano, Hawaii. Also, D. P. Hill (personal communication, 1999) has observed deepening of hypocenters with time during some swarms at Long Valley caldera, California. The deeper events at the end of the autumn 1985 swarm may have occurred to accommodate crustal relaxation in the region below an intruded dike. If fluids played a role in the migration, the question becomes what types of fluids are likely to be found at the observed depths and locations?

[63] *Fournier and Pitt* [1985] suggested that there is adequate permeability to transport hydrostatically pressurized fluids within the caldera to ~ 4 –5 km depth. At high temperatures ($>350^\circ\text{C}$) the precipitation of minerals in fractures sufficiently decreases permeability to prevent circulation [Fournier and Pitt, 1985]. Regular fracturing from earthquakes is required to sustain permeability levels high enough for hydrothermal circulation.

[64] In high-temperature regimes such as within the Yellowstone caldera, the maximum depth of earthquakes

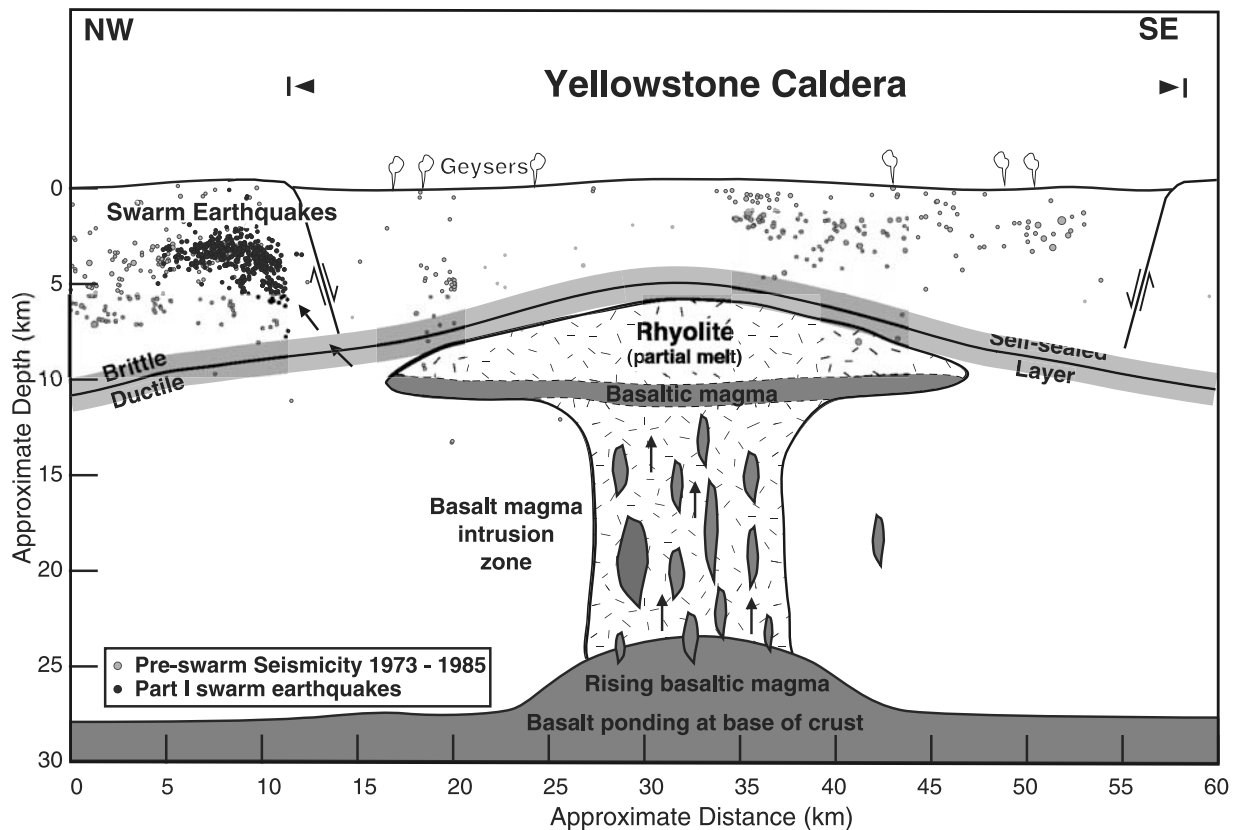


Figure 8. Plausible model of swarm triggering by migration of hydrothermal and/or magmatic fluids. This cartoon shows a path that fluids released from within a ruptured self-sealed layer or rhyolitic magma from a possible magma chamber, may have followed through the hot, ductile crust and into the a brittle fractured crust outside the caldera. The stress changes induced by the fluids generated earthquakes that migrated to the northwest with the fluids.

is an approximation for the depth of permeability [Fournier, 1989]. On the basis of this assumption and calculations of the depth of the base of the seismogenic zone by Smith *et al.* [1998], the maximum depth of penetration by meteoric water in the region of the autumn 1985 swarm is between ~8 and 9 km, near or below the base of the seismogenic zone. However, this assumption is probably only valid within the caldera where the heat flow is highest, and it is unlikely that meteoric waters penetrate to these depths.

[65] Another explanation is that these earthquakes occurred in response to the emplacement of magmatic or hydrothermal fluids above them during the first parts of the swarm. The fluid emplacement could modify the ambient stress field below it by decreasing the horizontal stress in the direction perpendicular to the dike. This would encourage normal faulting below the hypothesized dike, which agrees with the postswarm stress inversions. The lobe of solutions with a more vertically oriented σ_1 and R values higher than during the swarm reflects a return to normal faulting in the postswarm earthquakes.

[66] Finally, we note that this vertical migration may not be significant in terms of the errors in the hypocenter locations. We determined a rate of downward propagation by binning the data in groups of 25, 50, and 100 earthquakes and computing the mean hypocentral depth for each group. Depending on which bin size was used, a least squares straight-line fit to the data revealed rates from 20

to 30 m/d and the overall change in mean depth was between 2 and 3 km. This is about the limit of the minimum estimated focal depth error of ± 1.1 km so the apparent vertical migration may be an artifact of location error.

7. Conclusions

[67] The largest historic earthquake swarm in the Yellowstone volcanic field was concomitant with unprecedented changes in caldera deformation and hydrothermal activity from 1985 through 1986. The same processes that caused the reversal in caldera deformation from uplift to subsidence may have been responsible for the migration of earthquake activity away from the caldera along the north-northwest striking vertical plane.

[68] We propose a working model in which the net loss in volume beneath the caldera necessary to cause subsidence was partially accommodated by the migration of hydrothermal or magmatic fluids out of the caldera toward the northwest. The increased horizontal fluid pressure induced a change in the stress field that activated small earthquakes as it migrated at a high angle to the least principal stress direction. The stress changes associated with the first part of the swarm may have triggered the $M_c 4.9$ event on 9 November.

[69] We were not able to define a unique explanation for the 1985 Yellowstone swarm, but the rate of activity

migration along a steeply dipping plane and the orientations of the principal stress axes are consistent with models of migration of magmatic or hydrothermal fluids. The most likely scenario involves the rupture of a self-sealed hydrothermal layer and subsequent migration of hydrothermal fluid through a preexisting fracture zone out of the caldera. If this is correct, it has important implications for hazards related to future swarm activity. A better understanding of the mechanisms of swarms in Yellowstone National Park is then essential for accurate volcanic hazard assessment.

[70] **Acknowledgments.** This work was funded in part by U.S. Geological Survey Volcano Hazards Program grants 98-HQ-AG-2001 and 1434-95-A-01295. The National Park Service cooperated in operating the Yellowstone seismograph network. Special thanks are given to Sue Nava of the University of Utah Seismograph Stations for assistance with the Yellowstone earthquake data, to John W. Gephart for the use of FMSI, and to David Hill and Ron Bruhn for assistance with the original manuscript. Timely and thorough reviews by Dan Dzurisin, Roger Denlinger, and Allan Rubin helped to clarify and improve the paper.

References

- Bache, T. C., D. G. Lambert, and T. G. Barker, A source model for the March 28, 1975, Pocatello Valley earthquake from time-domain modeling of teleseismic *P* waves, *Bull. Seismol. Soc. Am.*, **70**, 405–418, 1980.
- Carslaw, H. S., and J. C. Jaeger, *Conduction of Heat in Solids*, Oxford Univ. Press, New York, 1959.
- Chang, W.-L., and R. B. Smith, Integrated seismic hazard along the Wasatch Front, Utah, *Bull. Seismol. Soc. Am.*, in press, 2002.
- Christiansen, R. L., The Quaternary and Pliocene Yellowstone Plateau volcanic field of Wyoming, Idaho, and Montana, *U.S. Geol. Surv. Prof. Pap.*, **729-G**, 2001.
- Doser, D. I., Source parameters and faulting processes of the 1959 Hebgen Lake, Montana, earthquake sequence, *J. Geophys. Res.*, **90**, 4537–4556, 1985.
- Dzurisin, D., J. C. Savage, and R. O. Fournier, Recent crustal subsidence at Yellowstone caldera, Wyoming, *Bull. Volcanol.*, **52**, 247–270, 1990.
- Dzurisin, D., K. M. Yamashita, and J. W. Kleinman, Mechanisms of crustal uplift and subsidence at the Yellowstone caldera, Wyoming, *Bull. Volcanol.*, **56**, 261–270, 1994.
- Eaton, G. P., R. L. Christiansen, H. M. Iyer, A. M. Pitt, H. R. Blank Jr., I. Zietz, D. R. Mabey, and M. E. Gettings, Magma beneath Yellowstone National Park, *Science*, **188**, 787–796, 1975.
- Fournier, R. O., Geochemistry and dynamics of the Yellowstone National Park hydrothermal system, *Annu. Rev. Earth Planet. Sci.*, **17**, 13–53, 1989.
- Fournier, R. O., Hydrothermal processes related to movement of fluid from plastic into brittle rock in the magmatic-epithermal environment, *Econ. Geol.*, **94**, 1193–1212, 1999.
- Fournier, R. O., and A. M. Pitt, The Yellowstone magmatic-hydrothermal system, U.S.A., in *1985 International Symposium on Geothermal Energy: International Volume*, edited by C. Stone, pp. 319–327, Cal Central, Sacramento, Calif., 1985.
- Fournier, R. O., D. E. White, and A. H. Truesdell, Convective heat flow in Yellowstone National Park, in *Second United Nations Symposium on Development and Use of Geothermal Resources*, pp. 731–739, U.S. Govt. Print. Off., Washington, D. C., 1976.
- Gephart, J. W., and D. W. Forsyth, An improved method for determining the regional stress tensor using earthquake focal mechanism data: Application to the San Fernando earthquake sequence, *J. Geophys. Res.*, **89**, 9305–9320, 1984.
- Gudmundsson, A., L. B. Marinoni, and J. Marti, Injection and arrest of dykes: Implications for volcanic hazards, *J. Volcanol. Geotherm. Res.*, **88**, 1–13, 1999.
- Hill, D. P., A model for earthquake swarms, *J. Geophys. Res.*, **82**, 1347–1352, 1977.
- Hill, D. P., W. L. Ellsworth, M. J. S. Johnston, J. O. Langbein, D. H. Oppenheimer, A. M. Pitt, P. A. Reasenber, M. L. Sorey, and S. R. McNutt, The 1989 earthquake swarm beneath Mammoth Mountain, California: An initial look at the 4 May through 30 September activity, *Bull. Seismol. Soc. Am.*, **80**, 325–339, 1990.
- Holdahl, S. R., and D. Dzurisin, Time-dependent models of vertical deformation for the Yellowstone-Hebgen Lake Region, *J. Geophys. Res.*, **96**, 2465–2483, 1991.
- Hutchinson, R. A., Summary of felt earthquakes in Yellowstone National Park, 1985, in *Earthquake Catalog for the Yellowstone National Park Region: January 1, 1985 to December 31, 1985*, pp. 46–61, Univ. of Utah Seismogr. Stn., Salt Lake City, 1986.
- Jackson, S. M., I. G. Wong, G. S. Carpenter, D. M. Anderson, and S. M. Martin, Contemporary seismicity in the eastern Snake River Plain, Idaho based on microearthquake monitoring, *Bull. Seismol. Soc. Am.*, **83**, 680–695, 1993.
- Julian, B. R., and R. S. Cockerham, Mechanisms of the May 1980 earthquakes near Long Valley Caldera, California: Evidence for dike injection, *Earthquake Notes*, **54**, 88–89, 1982.
- Klein, F. W., P. Einarsson, and M. Wyss, The Reykjanes Peninsula, Iceland, earthquake swarm of September 1972 and its tectonic significance, *J. Geophys. Res.*, **82**, 865–889, 1977.
- Kumagai, H., T. Ohminato, M. Nakano, M. Ooi, A. Kubo, H. Inoue, and J. Oikawa, Very-long-period seismic signals and caldera formation at Miyake Island, Japan, *Science*, **293**, 687–690, 2001.
- Linde, A. T., K. Agustsson, I. S. Sacks, and R. Stefansson, Mechanism of the 1991 eruption of Hekla from continuous borehole strain monitoring, *Nature*, **365**, 737–740, 1993.
- Lomax, A., J. Virieux, P. Volant, and C. Berge-Thierry, Probabilistic earthquake location in 3D and layered models, in *Advances in Seismic Event Location*, edited by C. H. Thurber and N. Rabinowitz, pp. 101–134, Kluwer Acad., Norwell, Mass., 2000.
- Meertens, C. M., R. B. Smith, and C. M. Puskas, Crustal deformation of the Yellowstone caldera from campaign and continuous GPS surveys, 1987–2000 (abstract), *Eos Trans. AGU*, **81**(48), Fall Meet. Suppl., Abstract V22F-19, 2000.
- Miller, D. S., and R. B. Smith, *P* and *S* velocity structure of the Yellowstone volcanic field from local earthquake and controlled source tomography, *J. Geophys. Res.*, **104**, 15,105–15,121, 1999.
- Muffler, L. J. P., D. E. White, and A. H. Truesdell, Hydrothermal explosion craters in Yellowstone National Park, *Geol. Soc. Am. Bull.*, **82**, 723–740, 1971.
- Newhall, C. G., and D. Dzurisin, Historical unrest at large calderas of the world, *U.S. Geol. Surv. Bull.*, **1855**, 1108 pp., 1988.
- Pelton, J. R., and R. B. Smith, Contemporary vertical surface displacements in Yellowstone National Park, *J. Geophys. Res.*, **87**, 2745–2761, 1982.
- Pitt, A. M., and R. A. Hutchinson, Hydrothermal changes related to earthquake activity at Mud Volcano, Yellowstone National Park, Wyoming, *J. Geophys. Res.*, **87**, 2762–2766, 1982.
- Pitt, A. M., C. S. Weaver, and W. Spence, The Yellowstone Park earthquake of June 30, 1975, *Bull. Seismol. Soc. Am.*, **69**, 187–205, 1979.
- Reasenber, P., and D. Oppenheimer, FPFIT, FPLOT and FPPAGE: FORTRAN computer programs for calculating and displaying earthquake fault-plane solutions, *U.S. Geol. Surv. Open File Rep.*, **85-0739**, 109 pp., 1985.
- Rubin, A. M., Getting granite dikes out of the source region, *J. Geophys. Res.*, **100**, 5911–5929, 1995a.
- Rubin, A. M., Propagation of magma-filled cracks, *Annu. Rev. Earth Planet. Sci.*, **23**, 287–336, 1995b.
- Rubin, A. M., and D. Gillard, Dike-induced earthquakes: Theoretical considerations, *J. Geophys. Res.*, **103**, 10,017–10,030, 1998.
- Rubin, A. M., and D. D. Pollard, Origins of blade-like dikes in volcanic rift zones, in *Volcanism in Hawaii*, edited by R. W. Decker, T. L. Wright, and P. H. Stauffer, *U.S. Geol. Surv. Prof. Pap.*, **1350**, 1449–1470, 1987.
- Rubin, A. M., D. Gillard, and J.-L. Got, A reinterpretation of seismicity associated with the January 1983 dike intrusion at Kilauea Volcano, Hawaii, *J. Geophys. Res.*, **103**, 10,003–10,015, 1998.
- Sasaki, S., Characteristics of microseismic events induced during hydraulic fracturing experiments at the Hijiori hot dry rock geothermal energy site, Yamagata, Japan, *Tectonophysics*, **289**, 171–188, 1998.
- Savage, J. C., M. Lisowski, W. H. Prescott, and A. M. Pitt, Deformation from 1973 to 1987 in the epicentral area of the 1959 Hebgen Lake, Montana, earthquake ($M_s = 7.5$), *J. Geophys. Res.*, **98**, 2145–2153, 1993.
- Simpson, D. W., W. S. Leith, and C. H. Scholz, Two types of reservoir-induced seismicity, *Bull. Seismol. Soc. Am.*, **78**, 2025–2040, 1988.
- Smith, R. B., and W. J. Arabasz, Seismicity of the Intermountain Seismic Belt, in *Neotectonics of North America*, edited by D. B. Slemmons, E. R. Engdahl, M. L. Zoback and D. D. Blackwell, pp. 185–228, Geol. Soc. of Am., Boulder, Colo., 1991.
- Smith, R. B., R. T. Shuey, R. Freidline, R. Otis, and L. Alley, Yellowstone hot spot: New magnetic and seismic evidence, *Geology*, **2**, 451–455, 1974.
- Smith, R. B., R. N. Harris, and D. S. Miller, Effect of high temperature on rheology and earthquakes in the Yellowstone volcanic field (abstract), *Eos Trans. AGU*, **79**(45), Fall Meet. Suppl., F976, 1998.
- Smith, R. P., S. M. Jackson, and W. R. Hackett, Paleoseismology and seismic hazards evaluations in extensional volcanic terrains, *J. Geophys. Res.*, **101**, 6277–6292, 1996.

- Talwani, P., and S. Acree, Pore pressure diffusion and the mechanism of reservoir-induced seismicity, *Pure Appl. Geophys.*, *122*, 947–965, 1985.
- Vasco, D. W., R. B. Smith, and C. L. Taylor, Inversion for sources of crustal deformation and gravity change at the Yellowstone caldera, *J. Geophys. Res.*, *95*, 19,839–19,856, 1990.
- Wells, D. L., and K. J. Coppersmith, New empirical relationships among magnitude, rupture length, rupture width, rupture area, and surface displacement, *Bull. Seismol. Soc. Am.*, *84*, 974–1002, 1994.
- Wicks, C., Jr., W. Thatcher, and D. Dzurisin, Migration of fluids beneath Yellowstone caldera inferred from satellite radar interferometry, *Science*, *282*, 458–462, 1998.
- Yosuke, A., P. Segall, T. Kato, P. Cervelli, and S. Shimada, Imaging magma transport during the 1997 seismic swarm off the Izu Peninsula, Japan, *Science*, *286*, 927–930, 1999.
- Zoback, M. L., State of stress and modern deformation of the northern Basin and Range Province, *J. Geophys. Res.*, *94*, 7105–7128, 1989.
- Zoback, M. L., First and second-order patterns of stress in the lithosphere: The World Stress Map Project, *J. Geophys. Res.*, *97*, 11,703–11,728, 1992.

R. B. Smith and G. P. Waite, Department of Geology and Geophysics, University of Utah, 1460 E. 135 S., Salt Lake City, UT 84112, USA. (rbsmith@mines.utah.edu; gpwaite@mines.utah.edu)

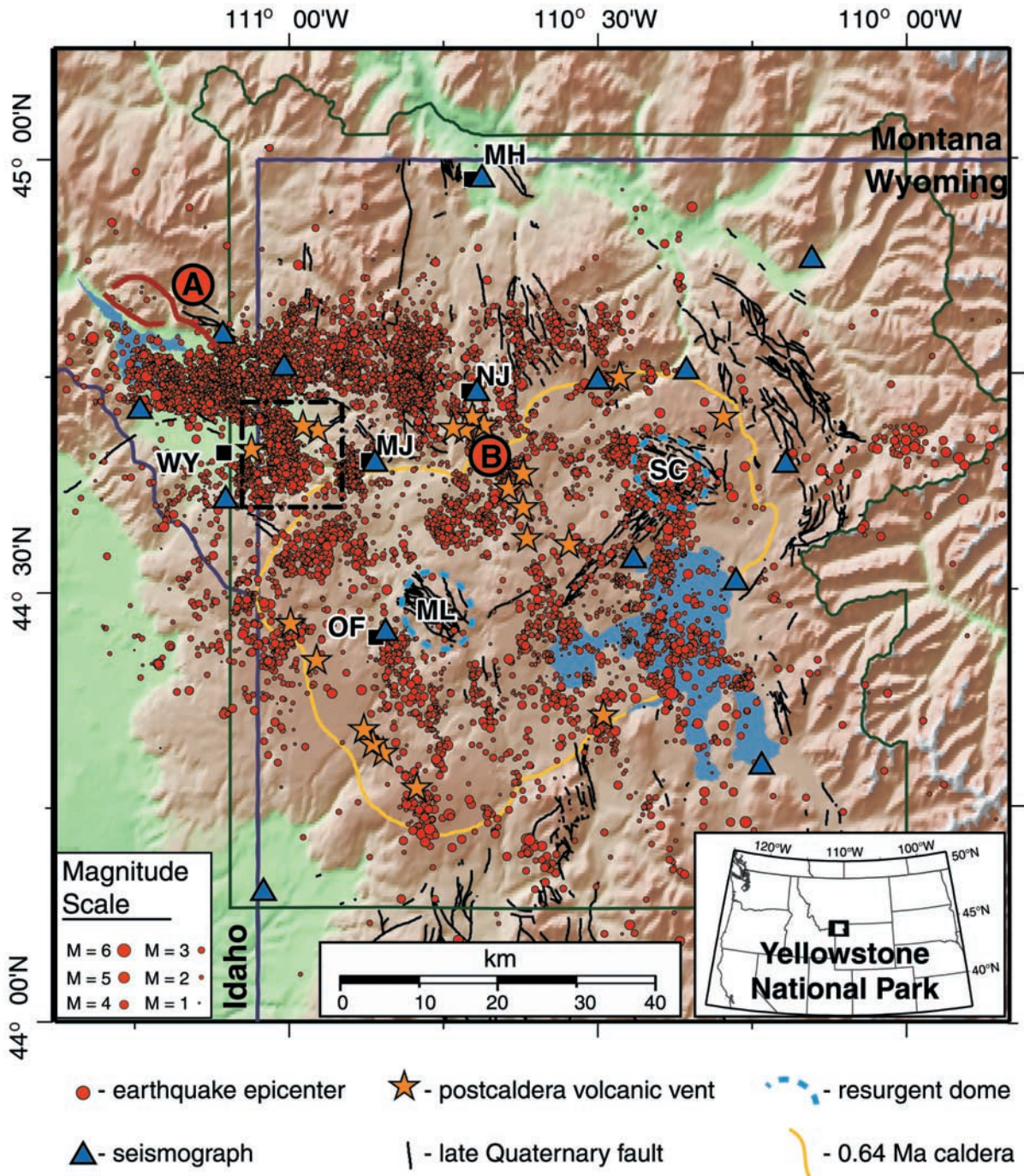


Figure 1. Yellowstone seismicity map: 1973–1997 (note that the network was not in operation from 1982 through late 1984). The Sour Creek (SC) and Mallard Lake (ML) resurgent domes are outlined with dashed blue lines. Place names are abbreviated MH, Mammoth Hotsprings; MJ, Madison Junction; NJ, Norris Junction; OF, Old Faithful; and WY, West Yellowstone. The rectangular region outlined with black is the region of the autumn 1985 swarm. Large circles mark the locations of the $M_S 7.5$ 1959 Hebgen Lake (A) and $M_L 6.1$ Norris Geyser basin (B) earthquakes. The surface rupture of the Hebgen Lake earthquake is shown as a maroon line. Figures 3 and 4 show the swarm sequence in more detail.

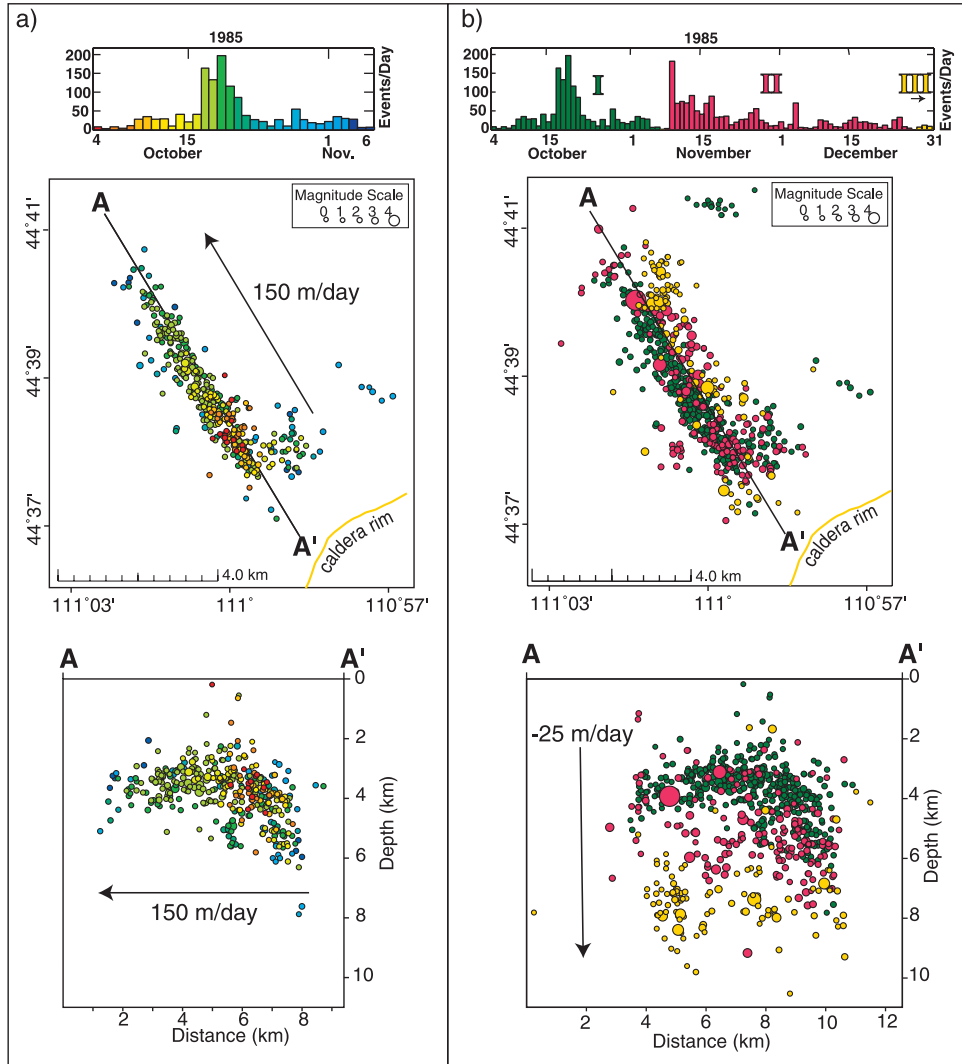


Figure 3. Earthquakes of the autumn 1985 Yellowstone swarm. Colors correspond to time periods shown in the bar graphs. (a) The initial month of the autumn 1985 earthquake swarm. Warm colors are earliest and cold colors are latest. Notice the general progression of the front of the swarm from southeast to northwest that is especially clear in the A-A' cross section with a 5-day flurry of activity beginning on 16 October. The rate of migration of activity is about 150 m/d. (b) All of the autumn 1985 swarm earthquakes. During the first month, shown in green, seismicity was relatively shallow. The red symbols correspond to the following month of activity during which events became systematically deeper. This second period began with two $M_C > 4$ events and decays similar to a main shock-aftershock sequence. The events shown in yellow continue on through 1986 in the same plane as the swarm and are the deepest. The downward migration occurred at a rate of about -25 m/d.